

Desorption and Exchange of Self-Assembled Monolayers (SAMs) on Gold Generated from Chelating Alkanedithiols

Young-Seok Shon and T. Randall Lee*

Department of Chemistry, University of Houston, Houston, Texas 77204-5641

Received: February 18, 2000; In Final Form: June 15, 2000

The kinetics of thermal desorption and displacement of self-assembled monolayers (SAMs) on gold derived from the adsorption of 2,2-dipentadecylpropane-1,3-dithiol (**d-C17**, $[\text{CH}_3(\text{CH}_2)_{14}]_2\text{C}[\text{CH}_2\text{SH}]_2$), 2-pentadecylpropane-1,3-dithiol (**m-C17**, $\text{CH}_3(\text{CH}_2)_{14}\text{CH}[\text{CH}_2\text{SH}]_2$), and heptadecanethiol (**n-C17**, $\text{CH}_3(\text{CH}_2)_{16}\text{SH}$) were explored. The kinetics were monitored by optical ellipsometry, contact angle goniometry, and polarization modulation infrared reflection absorption spectroscopy (PM-IRRAS). Thermal desorption studies of the SAMs in decalin at elevated temperatures demonstrated an enhanced stability for films generated from **d-C17** and **m-C17** relative to that for the film generated from **n-C17**. These studies further demonstrated that SAMs adsorbed at elevated temperatures (e.g., 50 °C) are more stable than those adsorbed at room temperature. Upon exposure to ambient laboratory conditions for one month, densely packed SAMs generated from **n-C17** and **d-C17** underwent no detectable structural changes. In contrast, similar treatment of the SAM generated from **m-C17**, which possesses a relatively low density of alkyl chains, led to structural change(s), as indicated by a progressive decrease in the values of the hexadecane contact angles. The data from the displacement studies suggest the following trend in the thermodynamic stabilities of the thiol-derived SAMs: **m-C17** > **d-C17** \gg **n-C17**. The degree of crystallinity of the alkyl chains of the SAMs failed to correlate with the observed trend in stabilities. The strong thermodynamic preference for **m-C17** and **d-C17** over **n-C17** probably originates from the unique ability of the former adsorbates to chelate to the surface of gold and perhaps their decreased tendency toward desorption as a disulfide. The slight thermodynamic preference for **m-C17** over **d-C17** probably originates from an enhanced conformational flexibility for **m-C17** that permits enhanced binding of this adsorbate to the surface of gold.

Introduction

The spontaneous adsorption of alkanethiols onto gold surfaces leads to the formation of structurally and chemically well-defined self-assembled monolayers (SAMs).^{1,2} Because SAMs are potentially useful in a number of technologies ranging from corrosion prevention^{3–5} and chemical sensing^{6,7} to biomaterials^{8,9} and microelectronic device fabrication,^{10–12} efforts directed toward enhancing the long-term stability of the films are drawing increasing emphasis. Although much evidence suggests that alkanethiolate SAMs exhibit moderate stabilities at room temperature,^{13,14} some reports suggest that SAMs desorb over the course of a few days upon exposure to air in the absence of light.^{15–17} Moreover, normal alkanethiol-based SAMs readily desorb upon heating to elevated temperatures (70 °C) in a hydrocarbon solvent¹⁸ and can be readily displaced from the surface by immersion in a solution containing a different thiol.^{18,19}

Because the poor stability of normal SAMs limits their usefulness in real world applications, many researchers have explored strategies for enhancing SAM stability. Some of these strategies include (1) the use of adsorbates having multiple sulfur–gold interactions,^{20–22} (2) the use of underpotential-deposited (UPD) metal substrates,^{23,24} and (3) the incorporation of “cross-linking” groups within the alkyl chains (i.e., hydrogen bonding, polymer precursor, or aromatic moieties).^{25–31} Much

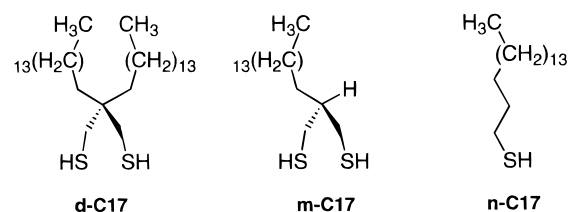


Figure 1. Structures of 2,2-dipentadecylpropane-1,3-dithiol (**d-C17**), 2-pentadecylpropane-1,3-dithiol (**m-C17**), and heptadecanethiol (**n-C17**).

of our current research is focused on the use of multiple sulfur–gold interactions to chelate to the surface of gold because we believe that the entropy-driven “chelate effect” should afford enhanced stabilities to SAM-based materials.^{32–34} Moreover, chelates can be designed³⁵ to resist the formation of intramolecular disulfides upon desorption from the surface,^{36,37} which should afford additional stability to the chelating SAMs. In previous reports,^{38–43} we described the preparation of chelating SAMs on gold from the adsorption of spiroalkanedithiol species such as those shown in Figure 1. Preliminary studies of thermal desorption in decalin suggested that these chelating SAMs are thermally more robust than normal SAMs on gold.³⁸ In this paper, we compare the thermal desorption profiles of the chelating SAMs to those of normal alkanethiol-based SAMs having similar chain lengths. We also compare the relative ease of displacement of chelating and normal alkanethiol-based SAMs.

* To whom correspondence should be addressed. E-mail: trlee@uh.edu.

Experimental Section

In previous reports,^{38,40} we described in detail many of the materials and experimental procedures used in the present study. Consequently, we provide here only a brief summary of supplementary details. Unless noted otherwise, SAMs were grown at room temperature by immersing gold-coated silicon wafers for 48 h in 1 mM solutions of the adsorbates (Figure 1) dissolved in isooctane. The resultant SAMs were immediately and thoroughly rinsed with toluene and ethanol and blown dry with ultrapure nitrogen. The kinetics of thermal desorption were monitored by immersing the SAM-coated wafers in hot decalin (also known as decahydronaphthalene or DHN) for the time intervals indicated on the kinetic plots. After the SAMs were washed thoroughly with ethanol and dried with a flow of nitrogen, ellipsometric thickness measurements were performed, and the samples were returned to the heated decalin solutions. Using a previously developed analytical method,^{18,23} relative ellipsometric thicknesses were used to calculate the fraction of SAM remaining on the surface. The stability of the films in air was monitored by contact angle goniometry and X-ray photoelectron spectroscopy (XPS) measurements. The kinetics of displacement were monitored by ellipsometry, hexadecane contact angle goniometry, and polarization modulation infrared reflection absorption spectroscopy (PM-IRRAS) upon immersion of the wafers in isooctane at 50 °C for the time intervals indicated on the kinetic plots. The total concentration of thiol-displacing agent(s) was maintained at 1 mM for both single-component and dual-component mixtures. The resultant SAMs were thoroughly rinsed with toluene and ethanol and blown dry with ultrapure nitrogen before analysis. Unless specified otherwise, the average values of ellipsometric thickness for at least 6 independent measurements were within ± 2 Å of those reported. Similarly, values of θ_a^{HD} were reproducible to within $\pm 2^\circ$ of those reported, and values of $\nu_a^{\text{CH}_2}$ were reproducible to within ± 1 cm^{-1} of those reported.

Results and Discussion

Thermal Desorption of SAMs at Elevated Temperatures.

We probed the thermal stability of the chelating SAMs by comparing the solution-phase desorption of the SAMs derived from 2,2-dipentadecylpropane-1,3-dithiol (**d-C17**) and 2-pentadecylpropane-1,3-dithiol (**m-C17**) to that of the analogous SAM derived from heptadecanethiol (**n-C17**). Figure 2 shows that, in decalin at temperatures ranging from 70 to 110 °C, the desorption profiles share at least two common features: (1) the data exhibit two different kinetic regimes of desorption, namely, a fast initial regime (steep slope) followed by a slower or nondesorbing regime (gentle slope); and (2) the rate and/or extent of desorption in both regimes increases with increasing temperature. At the lower temperature (70 °C), the SAM derived from **m-C17** appears to desorb faster than those derived from **d-C17** and **n-C17**. At higher temperatures (90 and 110 °C), however, the SAM derived from **n-C17** appears to desorb faster than the others. The variation of these trends with temperature was reproducible for at least two independently prepared samples.

Further analysis of the data in Figure 2 reveals that, after being heated for 1 h at 70 °C in decalin, $\sim 83\%$ of the SAM generated from **n-C17** remained on the surface, whereas only $\sim 73\%$ of the SAM generated from **d-C17** and $\sim 58\%$ of the SAM generated from **m-C17** remained on the surface. After being heated for longer times at 70 °C, however, the SAM derived from **d-C17** appeared to be the most resistant to desorption. For example, upon heating for 4 h at 70 °C, $\sim 59\%$

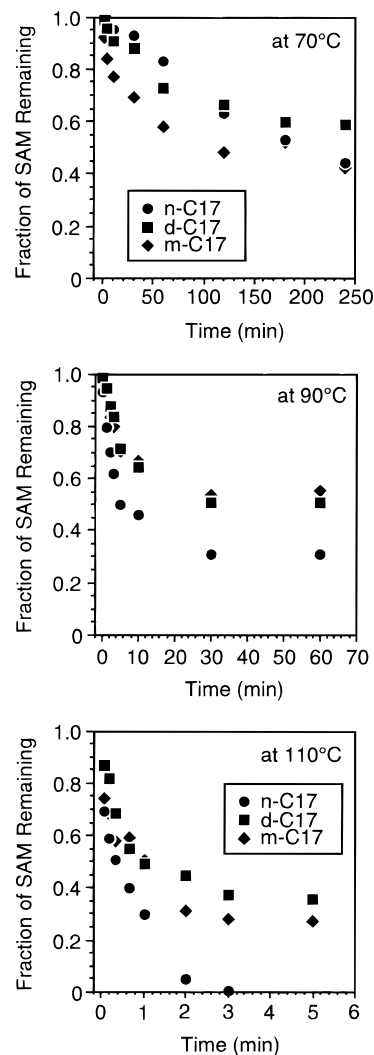


Figure 2. Thermal desorption profiles in decalin at 70, 90, and 110 °C for SAMs derived from the adsorption at room temperature of **n-C17** (●), **m-C17** (◆), and **d-C17** (■).

of the SAM derived from **d-C17** remained on the gold surface, whereas $\sim 44\%$ and $\sim 42\%$ of the SAMs derived from **n-C17** and **m-C17**, respectively, remained on the surface. Thermal desorption of the SAMs at 80 °C in decalin showed similar trends (data not shown).

As noted above, the profiles in Figure 2 collected at higher temperatures (i.e., >80 °C) show that the rates of desorption are faster for the SAMs generated from **n-C17** compared to those generated from **d-C17** and **m-C17**, whose rates of desorption are largely indistinguishable from each other. A detailed examination of these data reveals that, after being heated for 1 h at 90 °C in decalin, $\sim 51\%$ of the SAM generated from **d-C17** and $\sim 55\%$ of the SAM generated from **m-C17** remained on the surface, whereas only $\sim 31\%$ of the SAM generated from **n-C17** remained. Heating the SAMs at 100 and 110 °C in decalin afforded analogous but steeper desorption profiles.

Because the profiles collected at 70–80 °C suggested different relative stabilities than those collected at 90–110 °C, we questioned whether the SAMs generated by room temperature adsorption were thermodynamically equilibrated (i.e., whether the adsorption of **d-C17**, **m-C17**, and **n-C17** at room temperature afforded maximum packing densities and sulfur–gold interactions for each type of adsorbate). To test this hypothesis, we conducted the adsorptions at an elevated temperature (50 °C) and then examined the desorption behavior.

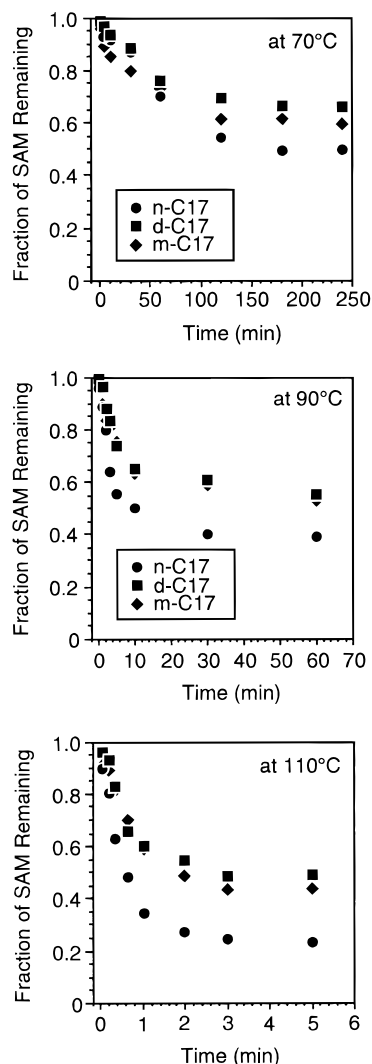


Figure 3. Thermal desorption profiles in decalin at 70, 90, and 110 °C for SAMs derived from the adsorption at 50 °C of **n-C17** (●), **m-C17** (◆), and **d-C17** (■).

The corresponding desorption profiles are shown in Figure 3. The apparent variation in relative stability with temperature was still evident, albeit diminished in magnitude. For example, the rates of desorption for all adsorbates were largely indistinguishable at 70 °C, but clearly faster for **n-C17** at 90 and 110 °C. Detailed examination of the data shows that, after being heated for 1 h at 70 °C in decalin, ~72% of the SAM generated from **n-C17** remained on the surface, whereas ~76% of the SAM generated from **d-C17** and ~73% of the SAM generated from **m-C17** remained on the surface. After being heated for 1 h at 90 °C in decalin, however, ~56% of the SAM generated from **d-C17** and ~48% of the SAM generated from **m-C17** remained on the surface, whereas only ~39% of the SAM generated from **n-C17** remained. Heating the SAMs at 110 °C in decalin afforded analogous but steeper desorption profiles when compared to those obtained at 90 °C.

In accord with previous reports of the solution-phase desorption of SAMs on gold,^{23,44,45} we analyzed the desorption profiles in Figures 2 and 3 by considering a fast initial desorption regime (characterized by a relatively steep slope) followed by a slow or nondesorbing regime (characterized by a relatively gentle slope). We note that, for alkanethiolate-based SAMs on polycrystalline gold, the adsorbates have been shown to desorb more readily from terrace sites than from step sites.⁴⁴ It is thus possible that multiple distinct binding sites on the surface give rise to

TABLE 1: First-Order Rate Constants (s^{-1}) for the Initial Desorption (Steep Slope) of SAMs Formed by Adsorption at 50 °C^a

adsorbate	k at 70 °C	k at 90 °C	k at 110 °C
n-C17	3.0×10^{-4}	3.7×10^{-3}	3.3×10^{-2}
m-C17	3.7×10^{-4}	2.5×10^{-3}	2.1×10^{-2}
d-C17	3.0×10^{-4}	2.2×10^{-3}	2.1×10^{-2}

^a In duplicate runs, the calculated values of the first-order rate constants were always within $\pm 10\%$ of those reported.

the distinct desorption regimes observed in the present work. In our analysis, we evaluated the rates of desorption in the fast regime (steep slope) by fitting the desorption data to first-order kinetics according to eq 1,

$$(T_t - T_\infty)/(T_0 - T_\infty) = e^{-kt} \quad (1)$$

where T_0 is the initial thickness of the SAM, T_t is the thickness of the SAM at time t , and T_∞ is the thickness of the slow/nondesorbing fraction of the SAM.⁴⁵ The thicknesses of the fractional SAM remaining were plotted versus time, and the first-order rate constants (k) were derived from the slope of the curves at the different temperatures.

Table 1 shows the initial rate constants for desorption in the fast regime at the various temperatures for the three types of SAMs examined here. We provide rate constants only for SAMs adsorbed at 50 °C because the data for SAMs adsorbed at room temperature yielded inconsistent results in this regime. The data in Table 1 illustrate two important features of the desorption behavior of the SAMs. First, the rate constants for initial desorption increase with increasing temperature, which is consistent with a thermally activated process.^{18,46} Second, the relative trend in the magnitude of the initial rate constants calculated for desorption at 70 °C is different from the trend for those at 90 and 110 °C. At 70 °C, the normal alkanethiol desorbs at similar or slower initial rates than the dithiols; at 90 and 110 °C, however, the normal alkanethiol desorbs at faster initial rates than the dithiols. This apparent variation in relative stability with temperature might be interpreted to indicate that the degree of crystallinity of the alkyl chains influences SAM stability at ambient temperatures²⁴ but not at elevated temperatures, where the films are probably more liquidlike.⁴⁷ It is perhaps more probable that the data simply reflect the chelate effect,^{32,33} whereby, at elevated temperatures, entropic factors would be expected to enhance the stability of the chelating adsorbates relative to that of normal alkanethiols on gold.³⁴

For the slow or nondesorbing regime (characterized by the gentle slope in the desorption profiles), we were unable to analyze *quantitatively* the kinetic data because of the relatively small changes in ellipsometric thickness and the relatively large error associated with the ellipsometric measurements. To provide, however, a *qualitative* measure of the relative stabilities of the SAMs in this regime, we chose to examine the time required for the desorption of an arbitrary fraction of the SAMs at a given temperature (i.e., ~50% at 90 °C). Figure 4 shows, for example, that the time required for 50% of the monolayer to desorb at 90 °C was greater for the SAMs derived from **d-C17** and **m-C17** than for the SAM derived from **n-C17**, regardless of whether the SAMs were formed at room temperature or at 50 °C.

There are at least four factors that might rationalize the enhanced stability of the dithiol-based SAMs (see Scheme 1). First, desorption of the dithiol-based SAMs requires the simultaneous (or nearly simultaneous) breaking of two S–Au bonds. Consequently, this entropy-driven chelate effect will be

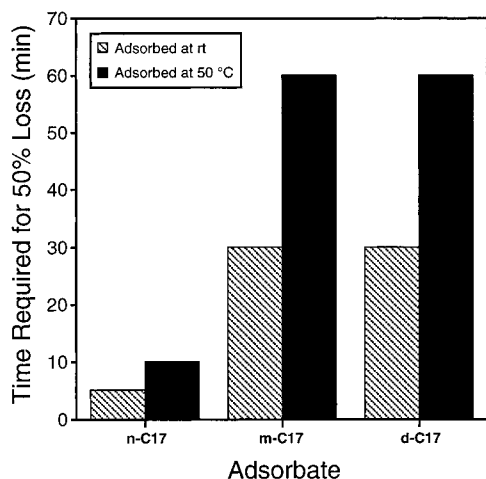
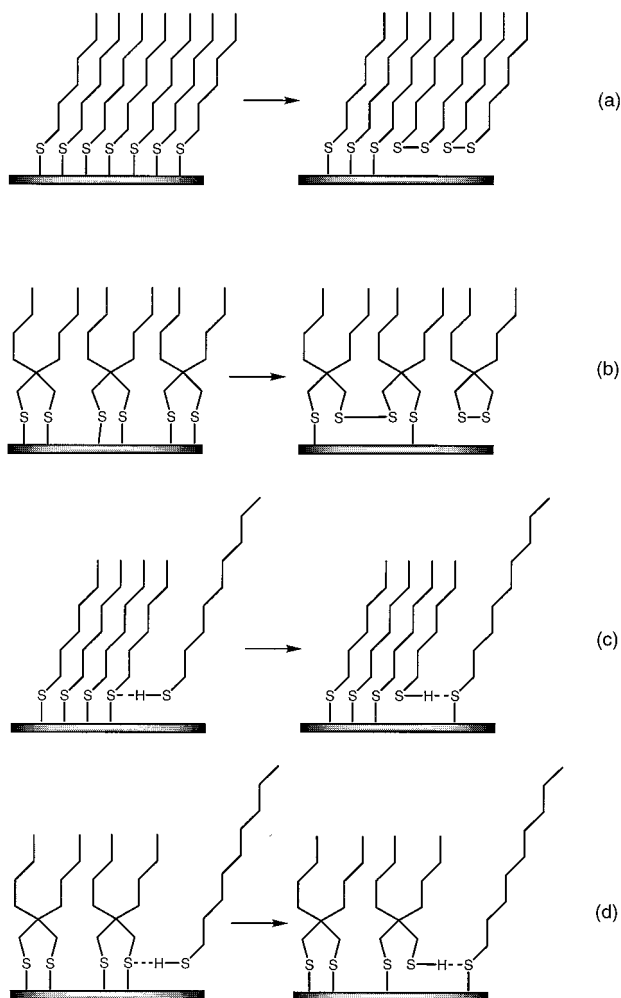


Figure 4. Time interval required for the desorption at 90 °C in decalin of ~50% of each SAM derived separately from the adsorptions of **n-C17**, **m-C17**, and **d-C17** at room temperature (rt) and at 50 °C in isooctane.

SCHEME 1: Proposed Mechanisms of Thermal Desorption and Displacement for SAMs Derived from n-C17, d-C17, and m-C17



expected to contribute to an enhanced stability for dithiol-based SAMs on gold.^{20,38} Second, given that alkanethiol-based SAMs on gold desorb from the surface as disulfides,^{48,49} *intramolecular* desorption of the chelating dithiols as cyclic disulfides (i.e., the dithiolanes shown in Scheme 1b)^{36,37} will be energetically disfavored because of ring strain generated in the products (~3.6

kcal/mol).³⁵ Third, pathways involving *intermolecular* desorption as disulfides are probably untenable, requiring the concurrent (i.e., entropically disfavored) desorption of four or more tethered sulfur atoms (see Scheme 1b). Fourth, if we consider multiple distinct binding sites on the surface of gold,⁴⁴ diffusion of some portion of the adsorbates on the surface from high-energy-barrier sites to low-energy-barrier sites is likely to occur prior to desorption.⁴⁵ Because the chelating dithiols bind to the surface via two sulfur atoms, diffusion on the surface is probably restricted for these adsorbates relative to that for normal alkanethiols on gold. This factor therefore might also contribute to an enhanced stability for the dithiol-based SAMs on gold.

Another interesting phenomenon that can be gleaned by comparing the adsorption profiles in Figure 2 to those in Figure 3 and by examining the relative stabilities of the SAMs as indicated by the data in Figure 4 is that the SAMs adsorbed at 50 °C are more resistant to desorption than those adsorbed at room temperature. To our knowledge, this type of stabilization, which appears to be a general characteristic for all three types of SAMs examined here, has been unreported until now. Our data are consistent with a model in which the adsorption at elevated temperatures leads to thermodynamically equilibrated and thus thermally robust SAMs on gold.

The thermal desorption profiles described in the preceding paragraphs are generally consistent with the results from the displacement studies described in the paragraphs below, despite the fact that the mechanism for thermal desorption of SAMs on gold might be different from that for displacement. Scheme 1 illustrates that the *thermal desorption* of SAMs on gold probably occurs via loss as a disulfide,^{36,37,48,49} whereas the *displacement* of SAMs on gold probably occurs via loss as a thiol.^{19,37}

Finally, we analyzed partially desorbed SAMs generated from **n-C17**, **d-C17**, and **m-C17** by PM-IRRAS and XPS to verify that the fractional coverages measured by ellipsometry correspond to residual organosulfur adsorbates rather than surface contaminants. We collected these data from samples desorbed at 90 °C for 30 min in decalin, which falls solidly within the slow/nondesorbing regimes for each type of adsorbate (see Figures 2 and 3). The data (not shown) were consistent with the presence of a partially adsorbed monolayer rather than adsorbed contaminants. For example, the methyl (ν^{CH_3}) and methylene (ν^{CH_2}) bands in the PM-IRRAS spectra were qualitatively less intense than those collected from SAMs at full coverage, and the antisymmetric methylene ($\nu_a^{\text{CH}_2}$) bands were shifted to higher wavenumber, which is consistent with the anticipated decrease in crystallinity for partially desorbed films. Analyses by XPS provided further support for partial SAM desorption by indicating the presence of carbon and bound sulfur (S 2p_{3/2} ~ 162 eV).⁵⁰ In addition, the **n-C17** SAM showed the greatest decrease in carbon coverage among the three SAMs, as judged by the increase in Au 4f intensities relative to data collected at full coverage.

Stability of SAMs in Air at Room Temperature. We examined the stability of the SAMs generated from **n-C17**, **d-C17**, and **m-C17** upon exposure to ambient laboratory air and light at room temperature. Table 2 shows that the SAMs generated from **n-C17** and **d-C17** are stable over the course of one month, as indicated by invariant ellipsometric thicknesses and contact angles of hexadecane. SAMs generated from **m-C17**, however, show a gradual decrease in the contact angles of hexadecane (34° → 12°). We also used XPS to monitor the stability of the films with time (data not shown). In particular, we examined the sulfur 2p region to explore the possible

TABLE 2: Values of Ellipsometric Thickness (Å) and Hexadecane Contact Angle (°) of Various SAMs as a Function of the Time Exposed to Air at Room Temperature^a

adsorbate	1 d	3 d	7 d	14 d	30 d
n-C17	19 (47°)	19 (47°)	19 (46°)	19 (46°)	19 (45°)
d-C17	19 (48°)	19 (47°)	19 (46°)	19 (45°)	19 (45°)
m-C17	16 (34°)	16 (30°)	14 (23°)	14 (19°)	14 (12°)

^a Ellipsometric thicknesses were reproducible to within ± 2 Å. Values of θ_a^{HD} for SAMs generated from **n-C17** and **d-C17** were reproducible to within $\pm 1^\circ$ of those reported; values for SAMs generated from **m-C17** varied more widely ($\pm 2^\circ$).

TABLE 3: Displacement of Preformed SAMs^a with Free Alkanethiols (1 mM in Isooctane) at Room Temperature for 24 h

SAMs	thickness	θ_a^{HD}	$\nu_a^{\text{CH}_2}$	reagents	thickness	θ_a^{HD}	$\nu_a^{\text{CH}_2}$
n-C17	19 ± 1	47	2919	n-C10	16 ± 2	37	2920
				d-C10	16 ± 1	41	2920
				m-C17	16 ± 1	38	2923
d-C17	19 ± 2	48	2921	n-C10	19 ± 1	46	2922
				d-C10	19 ± 1	45	2922
				m-C17	19 ± 1	46	2922
m-C17	15 ± 1	36	2924	n-C17	16 ± 1	34	2925
				d-C17	16 ± 1	36	2924

^a Preformed SAMs were generated by adsorption from isooctane at room temperature for 48 h. Values of θ_a^{HD} were reproducible to within $\pm 2^\circ$ of those reported. Values of $\nu_a^{\text{CH}_2}$ were reproducible to within ± 1 cm^{-1} of those reported.

oxidation of thiolates to sulfones or sulfonates.^{15,16} For all three types of SAMs, these studies showed no oxidized sulfur (BE > 165 eV) and no change in the S 2p_{3/2} binding energy after two weeks of storage under ambient laboratory conditions. Moreover, we calculated the relative carbon densities using a previously reported method⁴⁰ and found no change in the carbon coverage for any of the SAMs. These results suggest that the elemental composition of the adsorbates remains constant under these conditions.

Because the **m-C17** SAMs are disordered and possess loosely packed alkyl chains, the aforementioned decrease in contact angle for the **m-C17** SAM might arise from contamination by interdigitated organic impurities, although this hypothesis remains unsupported by the XPS studies. A structural rearrangement in which the loosely packed SAM exposes an increased fraction of methylene groups at the interface might also rationalize the observed decrease in the contact angles. In attempts to regenerate the initial state of the “degraded” **m-C17** SAMs, we reimmersed samples of the SAMs for 24 h in both isooctane and 1 M solutions of **m-C17** in isooctane. Subsequently measured contact angles of hexadecane suggested, however, that the “degradation” process was irreversible.

Displacement of Preformed SAMs. Because device fabrication strategies that utilize SAMs on gold often require the reimmersion of patterned SAMs into solutions of free alkanethiols,⁵⁰ the stability of preformed SAMs toward alkanethiol solutions remains an important factor in the reliability and performance of devices manufactured using these processes. To evaluate the relative ease of displacement of dithiol-based SAMs vs normal alkanethiol-based SAMs, we undertook a systematic series of SAM displacement experiments, which are presented in the following paragraphs.

Table 3 provides the results of the displacement of SAMs exposed to solutions of various adsorbates in isooctane for 24 h at room temperature. Immersion of SAMs derived from **n-C17** into solutions of decanethiol (**n-C10**) and 2,2-dioctylpropane-1,3-dithiol (**d-C10**) led to decreases in thickness (3 Å) and

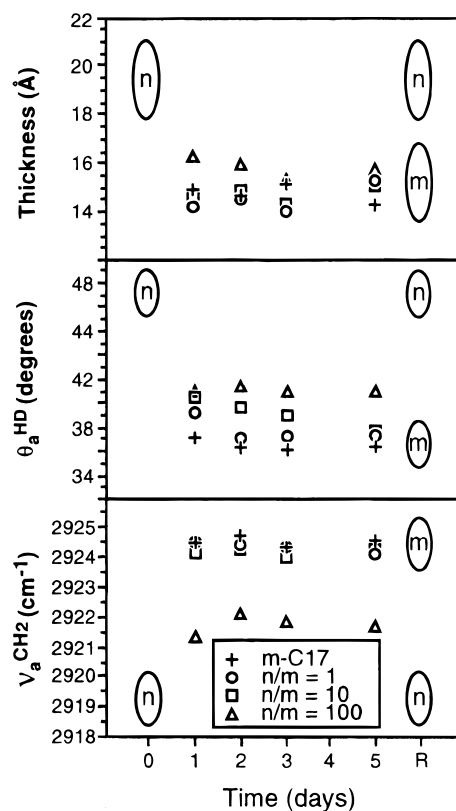


Figure 5. Displacement profiles for SAMs derived from **n-C17** upon exposure to isooctane solutions of pure **m-C17** and mixtures of **n-C17** and **m-C17** at ratios of **n-C17/m-C17** ranging from 1:1 to 100:1 at 50 °C. The total concentration of thiol displacing agent(s) was maintained at 1 mM. Limiting values for the **n-C17** SAM are provided at $t = 0$ (n); limiting values for the SAMs derived from the displacing agents (n and m) are provided at $t = R$.

hexadecane contact angles (10° and 6°, respectively). Analysis of the $\nu_a^{\text{CH}_2}$ band, which is particularly sensitive to the degree of conformational order (or crystallinity) of the films,⁵¹ showed a corresponding shift from 2919 to 2920 cm^{-1} , which is consistent with a slight decrease in crystallinity, but too small of a shift to be significant. Because the formation of mixed SAMs of normal alkanethiols having different chain lengths is known to expose the wettable, disordered methylene units of the longer adsorbate,^{52–54} the decreases in thickness and contact angle, when coupled with the small increase in the $\nu_a^{\text{CH}_2}$ band position, suggest that some fraction (but not all) of the **n-C17** monolayer was displaced by **n-C10** and by **d-C10**.⁵⁵ Complete displacement of the **n-C17** SAM by **n-C10** and by **d-C10** would be expected to afford limiting thicknesses of ~ 9 – 10 Å, hexadecane contact angles of ~ 41 – 46° , and $\nu_a^{\text{CH}_2}$ band positions of ~ 2923 – 2925 cm^{-1} . The displacement of the **n-C17** SAM by **m-C17** was, in contrast, more pronounced: comparable decreases in thickness and contact angle were accompanied by a significant shift in the $\nu_a^{\text{CH}_2}$ band position (2919 \rightarrow 2923 cm^{-1}), consistent with complete or nearly complete displacement of the **n-C17** SAM by **m-C17**.

In an analogous set of experiments, SAMs derived from **d-C17** were immersed in solutions of **n-C10**, **d-C10**, and **m-C17** at room temperature. The data in Table 3 show that, for all three displacement experiments, there was no detectable change in the ellipsometric thickness, a decrease in the hexadecane contact angle of only 2–3°, and a small but insignificant shift of the $\nu_a^{\text{CH}_2}$ band position. We note that, in this and the preceding set of displacement experiments, the relative chain lengths of the starting adsorbates (**n-C17** and **d-C17**) and the displacing agents

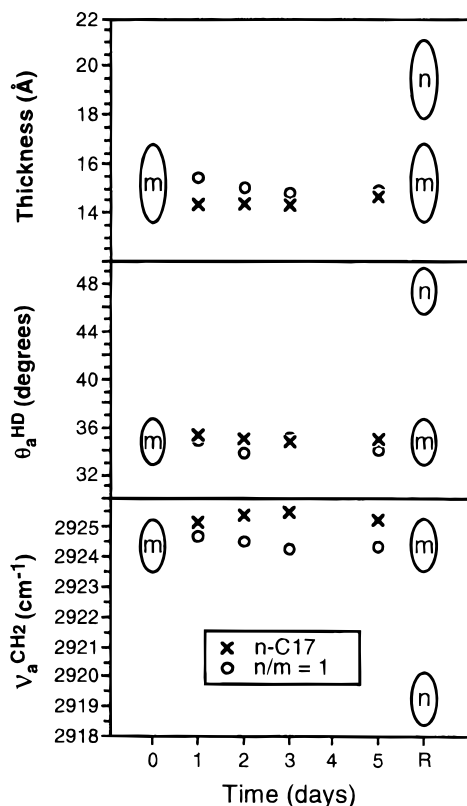


Figure 6. Displacement profiles for SAMs derived from **m-C17** upon exposure to isooctane solutions of pure **n-C17** and a 1:1 mixture of **n-C17** and **m-C17** at 50 °C. The total concentration of thiol displacing agent(s) was maintained at 1 mM. Limiting values for the **m-C17** SAM are provided at $t = 0$ (m); limiting values for the SAMs derived from the displacing agents (n and m) are provided at $t = R$.

(**n-C10** and **d-C10**) are analogous. Consequently, we can conclude from these data that, in the absence of solubility phenomena or other unknown effects, the **n-C17** SAM can be more readily displaced than the **d-C17** SAM.

We also explored the room-temperature displacement of the **m-C17** SAM upon exposure to solutions of **n-C17** and **d-C17** (Table 3). The data suggest that the **m-C17** SAM is remarkably resistant to displacement, as indicated by the invariance in the ellipsometric thicknesses, hexadecane contact angles, and $\nu_a\text{CH}_2$ band positions. These results are particularly surprising given that the alkyl chains of the SAMs generated from **m-C17** are disordered and possess a low density of alkyl chains,⁴⁰ which should afford ready access to the surface for displacing agents such as **d-C17** and particularly **n-C17**. Consequently, we can conclude from these studies that differences in the crystallinity of the alkyl chains (and the corresponding differences in interchain van der Waals interactions) are less important than other factors in dictating the relative ease of displacement of SAMs on gold. Given that both the **m-C17** and the **d-C17** SAMs are more resistant to displacement than the **n-C17** SAM and that the mechanism for displacement probably proceeds via desorption as thiol rather than disulfide,^{19,37} these results indicate that the chelate effect strongly enhances the stability of SAMs on gold.

Relative Thermodynamic Stability of SAMs from Displacement Studies. To establish that the data in Table 3 reflect thermodynamic rather than kinetic phenomena, we undertook a systematic series of displacement experiments (see Figures 5–10). In these experiments, we first generated the preformed SAMs by adsorption from solution at 50 °C for 48 h to ensure

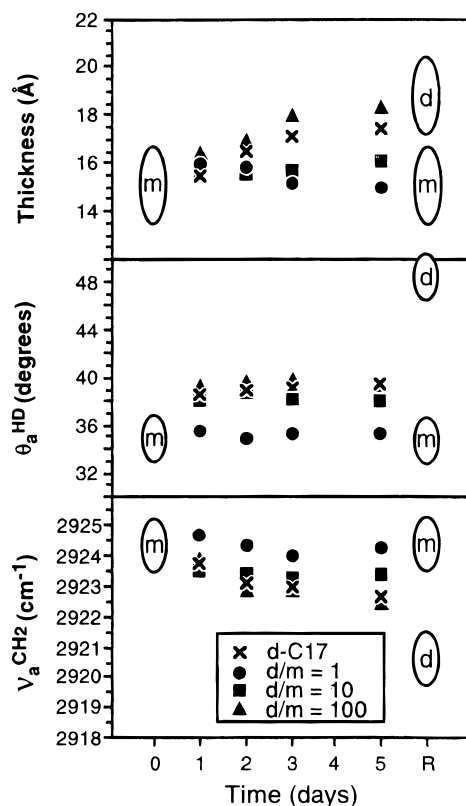


Figure 7. Displacement profiles for SAMs derived from **m-C17** upon exposure to isooctane solutions of pure **d-C17** and mixtures of **d-C17** and **m-C17** at ratios of **d-C17/m-C17** ranging from 1:1 to 100:1 at 50 °C. The total concentration of thiol displacing agent(s) was maintained at 1 mM. Limiting values for the **m-C17** SAM are provided at $t = 0$ (m); limiting values for the SAMs derived from the displacing agents (d and m) are provided at $t = R$.

that the starting SAMs were thermally equilibrated (vide supra). Second, we exposed the preformed SAMs to both single-component and dual-component solutions of displacing agents; in the latter solutions, we varied the ratios of the components, which typically contained some fraction of the starting adsorbate so that the data might reflect a true state of equilibrium for the SAMs. Third, we conducted the experiments at elevated temperatures (50 °C) over the course of several days until the data became invariant with time to ensure that the data would reflect a final state of equilibrium for the SAMs.

The plots in Figures 5–10 are constructed to show the limiting values of ellipsometric thickness, hexadecane contact angle, and $\nu_a\text{CH}_2$ band position of the preformed SAMs at $t = 0$. Progression to the right then illustrates the manner in which the properties of the SAMs vary with time. At the far right, the plots provide the limiting values of ellipsometric thickness, hexadecane contact angle, and $\nu_a\text{CH}_2$ band position for thermally equilibrated SAMs derived from independent adsorptions of the individual species used as the displacing agents; these species are identified in the box near the bottom of the plots. We then interpret the manner in which the data progress from left to right to indicate the final properties and thus the final compositions of the displaced SAMs.

Analysis of the data in Figure 5 reveals that the displacement of the **n-C17** SAM with a solution of pure **m-C17** occurs within 24 h. Exposure of the **n-C17** SAM to solutions containing 1:1 and 10:1 mixtures of **n-C17/m-C17** gives rise to the same conclusion. In contrast, however, exposure of the **n-C17** SAM to a solution containing a 100:1 mixture of **n-C17/m-C17** indicates partial, but nevertheless substantial, displacement.

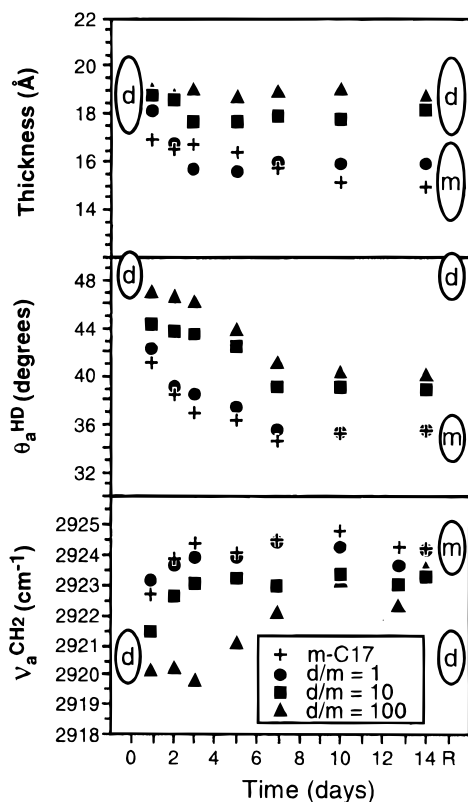


Figure 8. Displacement profiles for SAMs derived from **d-C17** upon exposure to isooctane solutions of pure **m-C17** and mixtures of **d-C17** and **m-C17** at ratios of **d-C17/m-C17** ranging from 1:1 to 100:1 at 50 °C. The total concentration of thiol displacing agent(s) was maintained at 1 mM. Limiting values for the **d-C17** SAM are provided at $t = 0$ (d); limiting values for the SAMs derived from the displacing agents (d and m) are provided at $t = R$.

These results demonstrate that the incorporation of **m-C17** is favored over that of **n-C17**. Figure 6 provides the converse study in which the **m-C17** SAM is exposed to solutions containing **n-C17** and a 1:1 mixture of **n-C17/m-C17**, neither of which appears to displace the **m-C17** SAM. The invariance of the data in Figure 6, when coupled with the changes observed in Figure 5, strongly suggests that the SAM derived from **m-C17** is more thermodynamically stable than that derived from **n-C17**.

To establish the relative stabilities of the **m-C17** and **d-C17** SAMs, we first explored the displacement of the **m-C17** SAM with solutions containing pure **d-C17** and mixtures of **d-C17** and **m-C17** (Figure 7). Exposure of the **m-C17** SAM to solutions containing pure **d-C17** and high ratios of **d-C17/m-C17** leads to the displacement of some portion of the **m-C17** SAM. Exposure to a 1:1 mixture of **d-C17** and **m-C17**, however, leads to no detectable displacement, which suggests a clear preference for the adsorption/retention of **m-C17**. Figure 8 provides the converse study in which the **d-C17** SAM is exposed to solutions containing pure **m-C17** and mixtures of **d-C17** and **m-C17**. Exposure of the **d-C17** SAM to all solutions containing **m-C17** leads to substantial, if not complete, displacement of the **d-C17** SAM. In particular, exposure to a 1:1 mixture of **m-C17** and **d-C17** appears to generate a pure **m-C17** SAM. Consequently, these data, when coupled with those in Figure 7 in which a 1:1 mixture of **d-C17/m-C17** affords no detectable displacement, strongly suggest that the SAM derived from **m-C17** is more thermodynamically stable than that derived from **d-C17**. The difference in stability between **m-C17** and **d-C17** SAMs, however, does not appear to be as substantial as that between **m-C17** and **n-C17** SAMs.

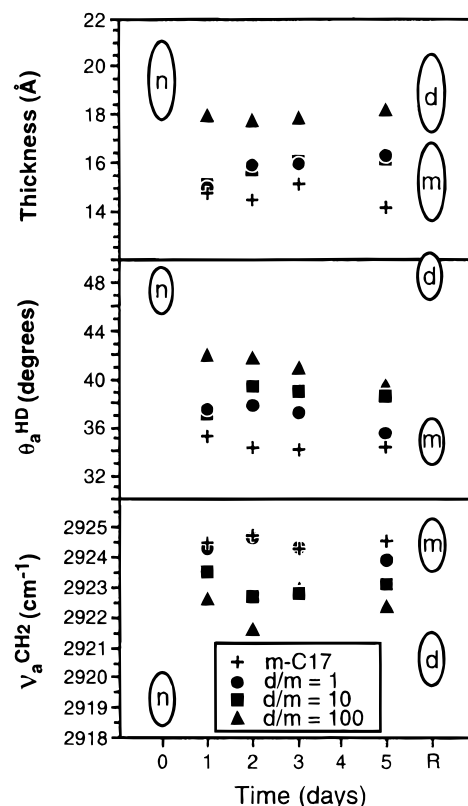


Figure 9. Displacement profiles for SAMs derived from **n-C17** upon exposure to isooctane solutions of pure **m-C17** and mixtures of **d-C17** and **m-C17** at ratios of **d-C17/m-C17** ranging from 1:1 to 100:1 at 50 °C. The total concentration of thiol displacing agent(s) was maintained at 1 mM. Limiting values for the **n-C17** SAM are provided at $t = 0$ (n); limiting values for the SAMs derived from the displacing agents (d and m) are provided at $t = R$.

Because of their nearly indistinguishable thicknesses, wettabilities, and IR spectra, direct displacement experiments between **n-C17** SAMs and **d-C17** (and the converse) would reveal little, if any, information regarding their relative thermodynamic stabilities. We felt, however, that by probing their displacement behaviors independently with **m-C17** and mixtures containing **m-C17**, we might nevertheless gain some insight regarding their relative stabilities. Figure 9 shows the displacement of the **n-C17** SAM with solutions containing pure **m-C17** and mixtures of **d-C17** and **m-C17**. The data show qualitatively the same behavior as in Figure 5; namely, that **m-C17** adsorbs preferentially on the surface. Slight differences between the profiles in Figures 5 and 7 (particularly at high **d-C17/m-C17** ratios) suggest, however, that facile displacement by **m-C17** appears to be marginally retarded by the presence of **d-C17**. Consequently, it appears that **d-C17** might compete more effectively with **m-C17** than does **n-C17** in the displacement of the **n-C17** SAM on gold.

In a final set of experiments, we compared the displacement of the **d-C17** SAM with solutions containing pure **m-C17** and mixtures of **n-C17** and **m-C17** (Figure 10). These studies demonstrate a clear preference for the adsorption of **m-C17**, although the kinetics of displacement are slower than those of the corresponding displacement of the **n-C17** SAM (see Figures 5 and 9). These studies thus indicate that **n-C17** is unable to effectively compete with **m-C17** in the displacement of pre-formed SAMs on gold.

Taken together, the data from the displacement studies suggest the following trend in the thermodynamic stabilities of the SAMs: **m-C17** > **d-C17** \gg **n-C17**. A plausible interpretation

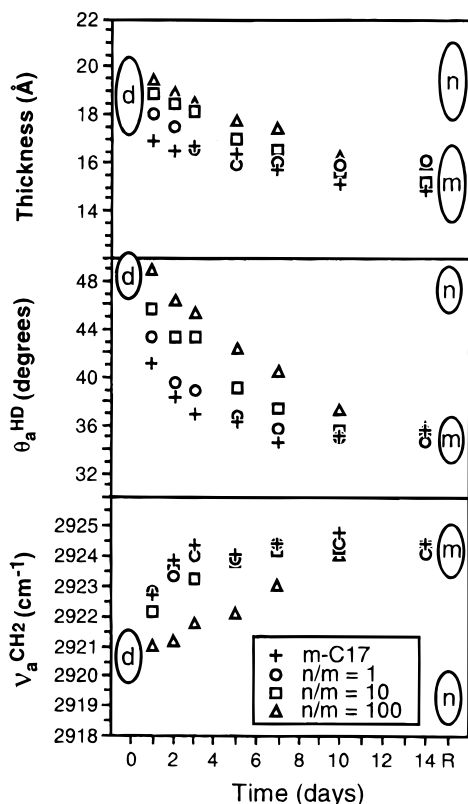


Figure 10. Displacement profiles for SAMs derived from **d-C17** upon exposure to isooctane solutions of pure **m-C17** and mixtures of **n-C17** and **m-C17** at ratios of **n-C17/m-C17** ranging from 1:1 to 100:1 at 50 °C. The total concentration of thiol displacing agent(s) was maintained at 1 mM. Limiting values for the **d-C17** SAM are provided at $t = 0$ (d); limiting values for the SAMs derived from the displacing agents (n and m) are provided at $t = R$.

for the enhanced thermodynamic stability of **m-C17** and **d-C17** vs that of **n-C17** lies in the chelate effect, as described above. Ring-strain effects that retard the desorption of the chelating adsorbates as cyclic disulfides might also contribute to an enhanced stability for the chelating SAMs. Other factors, such as differences in the solubility of the adsorbates, probably play a lesser role.⁵³ Because the SAM derived from **m-C17** is less densely packed than those derived from **n-C17** and **d-C17**,⁴⁰ the greater thermodynamic stability of **m-C17** vs the other adsorbates clearly outweighs any effects arising from differences in the interchain van der Waals stabilization of the SAMs. We propose that the thermodynamic preference for **m-C17** arises not only from the chelate effect, but also from an enhanced conformational⁴³ accessibility that allows for particularly strong binding to the surface of gold.

Conclusions

Studies of the thermal desorption in decalin of SAMs derived from **n-C17**, **d-C17**, and **m-C17** demonstrated that the latter two SAMs are more resistant to desorption than the SAM derived from **n-C17**. These studies further demonstrated that SAMs adsorbed at elevated temperatures (i.e., 50 °C) are more resistant to desorption than those adsorbed at room temperature. Analysis of partially desorbed SAMs generated from **n-C17**, **d-C17**, and **m-C17** by PM-IRRAS and XPS verified that the experimentally observed fractional coverages correspond to residual organosulfur adsorbates rather than surface contaminants. Other studies found that well-packed SAMs, such as those generated from **n-C17** and **d-C17**, are stable in air for more

than one month; in contrast, however, the loosely packed SAM generated from **m-C17** undergoes an undefined structural change over the course of one month. Displacement studies suggested the following trend in the thermodynamic stabilities of the SAMs: **m-C17** > **d-C17** \gg **n-C17**. The degree of crystallinity of the alkyl chains of the SAMs failed to correlate with the relative stabilities of the films. The thermodynamic preference for **m-C17** and **d-C17** over **n-C17** was rationalized on the basis of the chelate effect and related entropic considerations that afford additional stability to the **m-C17** and **d-C17** SAMs. Ring strain generated in the formation of the cyclic disulfide desorption products might also contribute to the enhanced stability of the chelating SAMs. The greater thermodynamic stability of **m-C17** vs **d-C17** probably arises from an enhanced conformational accessibility for **m-C17** that permits this adsorbate to bind particularly strongly to the surface of gold.

Acknowledgment. The National Science Foundation (CAREER Award to T.R.L.; CHE-9625003) and the Robert A. Welch Foundation (Grant E-1320) provided generous support for this research. We thank our colleague Jonathan Friedman for many helpful discussions.

References and Notes

- Ulman, A. *Thin Films—Self-Assembled Monolayers of Thiols*; Academic Press: Boston, MA, 1998.
- Whitesides, G. M.; Laibinis, P. E. *Langmuir* **1990**, *6*, 87.
- Zamborini, F. P.; Campbell, J. K.; Crooks, R. M. *Langmuir* **1998**, *14*, 640.
- Zamborini, F. P.; Crooks, R. M. *Langmuir* **1998**, *14*, 3279.
- Jennings, G. K.; Munro, J. C.; Yong, T.-H.; Laibinis, P. E. *Langmuir* **1998**, *14*, 6130.
- Crooks, R. M.; Ricco, A. J. *Acc. Chem. Res.* **1998**, *31*, 219.
- Ishihara, T.; Higuchi, M.; Takagi, T.; Ito, M.; Nishiguchi, H.; Takita, Y. *J. Mater. Chem.* **1998**, *8* (9), 2037.
- Heleg-Shabtai, V.; Katz, E.; Willner, I. *J. Am. Chem. Soc.* **1997**, *119*, 8121.
- Katz, E.; Heleg-Shabtai, V.; Willner, I.; Rau, H. K.; Haehnel, W. *Angew. Chem., Int. Ed. Engl.* **1998**, *37*, 3253.
- Hickman, J. J.; Ofer, D.; Laibinis, P. E.; Whitesides, G. M.; Wrighton, M. S. *Science* **1991**, *252*, 688.
- Abbott, N. L.; Rolison, D. R.; Whitesides, G. M. *Langmuir* **1994**, *10*, 2672.
- Gardner, T. J.; Frisbie, C. D.; Wrighton, M. S. *J. Am. Chem. Soc.* **1995**, *117*, 6927.
- Laibinis, P. E.; Whitesides, G. M. *J. Am. Chem. Soc.* **1992**, *114*, 9022.
- Kumar, A. K.; Biebuyck, H. A.; Whitesides, G. M. *Langmuir* **1994**, *10*, 1498.
- Schoenfish, M. H.; Pemberton, J. E. *J. Am. Chem. Soc.* **1998**, *120*, 4502.
- Lee, M.-T.; Hsueh, C.-C.; Freund, M. S.; Ferguson, G. S. *Langmuir* **1998**, *14*, 6419.
- Scott, J. R.; Baker, L. S.; Everett, W. R.; Wilkins, C. L.; Fritsch, I. *Anal. Chem.* **1997**, *69*, 2636.
- Bain, C. D.; Troughton, E. B.; Tao, Y.-T.; Evall, J.; Whitesides, G. M.; Nuzzo, R. G. *J. Am. Chem. Soc.* **1989**, *111*, 321.
- Schlenoff, J. B.; Li, M.; Ly, H. *J. Am. Chem. Soc.* **1995**, *117*, 12528.
- Garg, N.; Lee, T. R. *Langmuir* **1998**, *14*, 3815.
- Whitesell, J. K.; Chang, H. K. *Science* **1993**, *261*, 73.
- Wooster, T. T.; Gamm, P. R.; Geiger, W. E.; Oliver, A. M.; Black, A. J.; Graig, D. C.; Paddon-Row, M. N. *Langmuir* **1996**, *12*, 6616.
- Jennings, G. K.; Laibinis, P. E. *Langmuir* **1996**, *12*, 6173.
- Jennings, G. K.; Laibinis, P. E. *J. Am. Chem. Soc.* **1997**, *119*, 5208.
- Clegg, R. S.; Hutchison, J. E. *Langmuir* **1996**, *12*, 5239.
- Clegg, R. S.; Reed, S. M.; Hutchison, J. E. *J. Am. Chem. Soc.* **1998**, *120*, 2486.
- Batchelder, D. N.; Evans, S. D.; Freeman, T. L.; Häussling, L.; Ringsdorf, H.; Wolf, H. *J. Am. Chem. Soc.* **1994**, *116*, 1050.
- Kim, T.; Chan, K. C.; Crooks, R. M. *J. Am. Chem. Soc.* **1997**, *119*, 189.
- Ford, J. F.; Vickers, T. J.; Mann, C. K.; Schlenoff, J. B. *Langmuir* **1996**, *12*, 1944.
- Cai, M.; Mowery, M. D.; Menzel, H.; Evans, C. E. *Langmuir* **1999**, *15*, 1215.

- (31) Tao, Y.-T.; Wu, C.-C.; Eu, J.-Y.; Lin, W.-L. *Langmuir* **1997**, *13*, 4018.
- (32) Purcell, K. F.; Kotz, J. C. *Inorganic Chemistry*; W. B. Saunders: Philadelphia, PA, 1977.
- (33) Huheey, J. E. *Inorganic Chemistry*; Harper Collins: Singapore, 1983.
- (34) For ligand–metal interactions in organometallic complexes, the chelate effect contributes on the order of $\Delta G \sim -4$ kcal/mol of stabilization at room temperature [i.e., $\Delta H \sim -2$ kcal/mol and $\Delta S \sim +7$ cal/(K mol)].^{45,46} Because ΔS is positive, the chelate effect becomes more pronounced with increasing temperature.
- (35) Burns, J. A.; Whitesides, G. M. *J. Am. Chem. Soc.* **1990**, *112*, 6296.
- (36) Biebuyck, H. A.; Whitesides, G. M. *Langmuir* **1993**, *9*, 1766.
- (37) Kolega, R. R.; Schlenoff, J. B. *Langmuir* **1998**, *14*, 5469.
- (38) Shon, Y.-S.; Lee, T. R. *Langmuir* **1999**, *15*, 1136.
- (39) Shon, Y.-S.; Garg, N.; Colorado, R., Jr.; Villazana, R. J.; Lee, T. R. *Mater. Res. Soc. Symp. Proc.* **1999**, *576*, 183.
- (40) Shon, Y.-S.; Colorado, R., Jr.; Williams, C. T.; Bain, C. D.; Lee, T. R. *Langmuir* **2000**, *16*, 541.
- (41) Lee, S.; Shon, Y.-S.; Colorado, R., Jr.; Guenard, R. L.; Lee, T. R.; Perry, S. S. *Langmuir* **2000**, *16*, 2220.
- (42) Shon, Y.-S.; Lee, S.; Perry, S. S.; Lee, T. R. *J. Am. Chem. Soc.* **2000**, *122*, 1278.
- (43) Shon, Y.-S.; Lee, T. R. *J. Phys. Chem. B* **2000**, *104*, 8182.
- (44) Walczak, M. M.; Alves, C. A.; Lamp, B. D.; Porter, M. D. *J. Electroanal. Chem.* **1995**, *396*, 103.
- (45) Garg, N.; Carrasquillo-Molina, E.; Lee, T. R. *Langmuir*, manuscript submitted.
- (46) Dubois, L. H.; Zegarski, B. R.; Nuzzo, R. G. *J. Am. Chem. Soc.* **1990**, *112*, 570.
- (47) Bensebaa, F.; Ellis, T. H.; Badia, A.; Lennox, R. B. *Langmuir* **1998**, *14*, 2361.
- (48) Nishida, N.; Hara, M.; Sasabe, H.; Knoll, W. *Jpn. J. Appl. Phys.* **1996**, *35*, L799.
- (49) Nuzzo, R. G.; Zegarski, B. R.; Dubois, L. H. *J. Am. Chem. Soc.* **1987**, *109*, 733.
- (50) Tien, J.; Terfort, A.; Whitesides, G. M. *Langmuir* **1997**, *13*, 5349.
- (51) Nuzzo, R. G.; Dubois, L. H.; Allara, D. L. *J. Am. Chem. Soc.* **1990**, *112*, 558.
- (52) Bain, C. D.; Whitesides, G. M. *J. Am. Chem. Soc.* **1989**, *111*, 7164.
- (53) Shon, Y.-S.; Lee, S.; Perry, S. S.; Lee, T. R. *J. Am. Chem. Soc.* **2000**, *122*, 1278.
- (54) Shon, Y.-S.; Lee, S.; Perry, S. S.; Lee, T. R. *J. Am. Chem. Soc.*, web release date: July 19, 2000.
- (55) Because interchain interactions (e.g., van der Waals forces) in SAMs on gold increase with increasing chain length of the adsorbates,^{49,52} the displacement of a long-chain alkanethiolate with a short-chain alkanethiol should be less favored than the converse. However, in isooctane, the thermodynamic discrimination between long-chain and short-chain thiols will be much smaller than that in polar solvent systems such as ethanol.⁵²